Materials Research, Vol. 6, No. 1, 57-61, 2002.

Boron Doped Diamond Thin Films on Large Area Ti6Al4V Substrates for Electrochemical Application

Alessandra V. Diniz[a,b]*, *Neidenêi G. Ferreira*[a], *Evaldo J. Corat*[a], *Vladimir J. Trava-Airoldi*[a]

[a]*Instituto Nacional de Pesquisas Espaciais, INPE, Av. dos Astronautas, 1758, C.P. 515 12201-970, São José dos Campos - SP, Brazil*
[b]*Instituto Tecnológico de Aeronáutica, ITA São José dos Campos - SP, Brazil*

Received: January 02, 2002; Revised: September 30, 2002

Boron doped diamond thin films were grown on titanium alloy substrates (Ti6Al4V) with 36 × 35 × 1.3 mm at 873-933 K at 6.5 × 10^3 Pa during 8 h by hot filament CVD assisted technique. The boron source was obtained from a H_2 line forced to pass through a bubbler containing B_2O_3 dissolved in methanol (B\C = 6000 ppm). The films were grown on both sides of perforated and non-perforated substrates. Emphasis for diamond growing on perforated substrates have been done in order to increase the active surface area and hereafter to promote an easier electrolyte flow for wastewater treatment. The electrode performance was determined by cyclic voltammetry measurements in KCl, KNO_3, Na_2SO_4, HCl, HNO_3 and H_2SO_4 solutions and the reversibility behavior of the $Fe(CN)_6^{3-/4-}$ at the Ti6Al4V/Diamond electrode were studied. Also, Scaning Electron Microcopy and Raman Scattering Spectroscopy were used for morphology and diamond quality evaluation, respectively.

Keywords: *boron doped-diamond, Ti6Al4V, electrochemistry*

1. Introduction

The evolution of semiconductor diamond research has shown promising results with doping process during CVD growth. The standard methods used for CVD boron doped diamond were initially thermal diffusion and ion implantation[1,2]. These processes were made *ex situ*, after the film growth, and the no contamination of the growth reactor is the main advantage. However, alternative techniques have shown highly doped films, using *in situ* process from a solid source of boron inside of the reactor[3] and by introducing of B_2O_3 in a methanol-acetone mixture[4]. It was observed better results evidenced by more homogeneity in films bulk, also showing films with a linear relation between the doping levels and boron concentration in the precursor source.

The diamond electrodes, which correspond to a typical p-type semiconductor, offer high sensitivity, good precision and high stability when compared with vitreous carbon, for example. Its more remarkable property is a wide working potential window concerning to hydrogen and oxygen evolution in aqueous solutions. Consequently, this kind of electrodes can withstand corrosive environments and favor alternative reactions[5].

The main used substrate was the Si once its presents good characteristics for many applications. More recently, titanium alloy substrate became a good alternative for diamond growth since they have higher mechanical strength and electrical conductivity[6]. However some problems related to diamond film delamination became a goal to be overcome. It usually occurs due to the generation of high residual stresses in both films and substrate. Thermal stresses are often high in diamond films as a result of high deposition temperatures and the low thermal expansion coefficient of diamond compared to Ti6Al4V[7]. Some solutions for this problem have been found, as the low deposition temperature and stress relieves by slow temperature dropping, and have been considered in this work. Also, an electrochemical investigation for characterization of boron-doped diamond electrodes on Ti6Al4V is one of the purposes of this work. We have carried out electrochemical experiments provid-

*e-mail: avdiniz@las.inpe.br

ing voltammetric behavior studies for diamond electrodes in different neutral and acid solutions, and in 1 mM of ferrocyanide at scan rates from 5 up to 500 mV/s. The morphology and films quality were analyzed by SEM and Raman spectroscopy.

2. Experimental Procedure

Depositions were performed using a tubular stainless steel HFCVD reactor 100 mm diameter with one H_2 line that passes through a bubbler containing B_2O_3 dissolved in methanol (B\C = 6000 ppm in solution, flux from the bubbler = 20 sccm), as has been described elsewhere[8].

Ti6Al4V 35 × 35 × 1,3 mm perforated and non-perforated samples has been used. The laser made perforation increased geometric area by approximately 95%.

All samples were ground using 600 and 1000 SiC papers successively and polished using 9T and 5T Al_2O_3 powder, and then ultrasonically prepared in hexane bath with 0,25 μm diamond powder for 1 h.

The films were grown in both sides of the substrates with the aid of a tripod. The temperature and pressure were 900 ± 25 K and 6.5 × 10^3 Pa respectively. The total gas flow was kept constant at 100 sccm during 8 h with gas mixture of 1.0% vol. of methane in hydrogen, plus the B_2O_3 in methanol. The reactor has a rotative mechanism for the substrate that provides better uniformity during film growth. After the growth period the Ti6Al4V/diamond were cooled down to room temperature continually during 4 h.

The non-perforated electrodes were assembled over a brass base and electrical contact was made with a silver-based paste to the rear side of the substrate. The group was isolated with silicone wax inside a Teflon box. The electrodes did not have surface pre-treatment before the electrochemical measurements.

Electrochemical activity of the diamond/Ti6Al4V and diamond/silicon electrodes was analyzed in 0.1 M of neutral (KCl, Na_2SO_4 and $NaNO_3$) and acidic (HCl, H_2SO_4 and HNO_3) solutions. The anodic and cathodic charge was evaluated from cyclic voltammety in 1mM of ferrocyanide/0.1 M KCl at scan rates from 5 up to 500 mV/s. The experiments were carried out at room temperature. The solution was exposed to air during electrochemical measurements. A conventional three-electrodes (work electrode, counter electrode and reference electrode), single-compartment electrochemical cell was used using a Microquímica potentiostat model MQPG-01. The solution was not stirred during the voltametry experiments. A reference electrode of Ag/AgCl was used in this study. A platinum foil was also used during all the electrochemical measurements as counter electrode.

The characterizations of the films morphology and diamond quality were made by a LEO 440 scanning electron microscopy system and by a Renishaw Microscope 2000 micro-Raman scattering system, respectively.

3. Results and Discussions

Scanning Electron Microscopy and Raman Spectroscopy

First of all, surface and quality analyses have been carried out. SEM analysis for boron-doped diamond films on Ti6Al4V is depicted in Fig. 1. It is observed a polycrystalline film with predominant (111) and (100) orientation also determinated by X-Ray analysis. The films grew on the surface (Fig. 1a) and on the border of the samples, as is shown in Fig. 1b. The grains are very twinned, with average size around 1μm for 1.3 μm film thickness, which was measured by SEM cross section. The thickness, the average grain size and the low growth rate are smaller in comparison with standard diamond electrodes on silicon[9]. This probably oc-

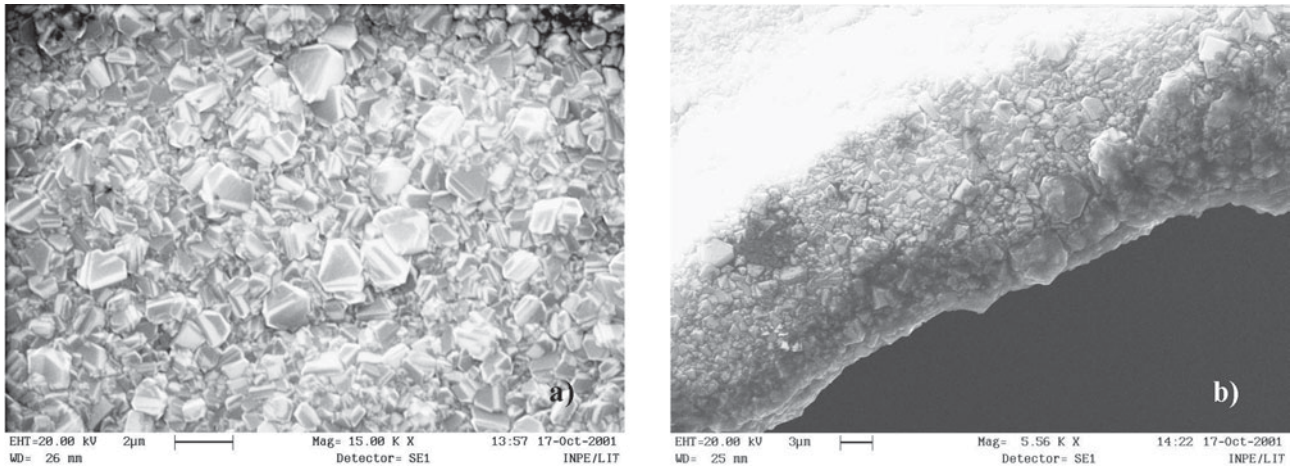

Figure 1. Scanning electron micrographs of boron-doped diamond film (a) superficial vision; (b) vision of the border of the sample.

curred due to the low deposition temperature[10] at 600 °C. This temperature seems to be best for diamond growth on Ti6Al4V considering the best benefits in terms of diamond quality and thermal stress component value for keeping an adherent film[11,12].

A TiC interlayer is formed between the diamond films and the Ti6Al4V as observed by X-Ray analysis. It is already know that at low temperature the titanium carbide interlayer has low growth rate and small thickness[7]. This characteristic favors the adhesion once the debonding occurs at the interface region between the TiC layer and the diamond film. Since the TiC formation is lower, the diamond formation is favored by available methane concentration in the gas phase, near the surface, and high nucleation rate is observed.

The Raman spectrum, as depicted in Fig. 2, shows a narrow sp^3 peak at 1340 cm^{-1} and a wide band centered at ~1550 cm^{-1}. The displacement and the splitting of the diamond characteristic peak (1332 cm^{-1} for natural diamond) is attribute to the high residual stress in the film, which Terranova *et al.*[13] also observed for diamond films on Ti6Al4V. This stress probably occurred due to the high mechanical resistance of the titanium alloys which could not allow a partial relaxation of the high thermal stress and the different compositions of the interfacial layers[14]. The positive shifts have to be interpreted as films in compressive stress[15].

The wide band centered at 1550 cm^{-1} is attributed to sp^2 carbons bond in the film[16]. This result was expected once the methane concentration around 2% is relatively higher than other values normally used[17]. As shown in Fig. 2a, this band is shifted, probably due to the small D band contribution[15] and high amorphous carbon concentration in the film. This effect can also be explained the low sp^3 characteristic peak intensity in this Raman spectrum.

Also, the Raman spectrum doesn't show a broad band centered at 1200 cm^{-1}, that result of the breakdown of the k = 0 selection rule, probably because of the films are only slightly doped[8,18,19].

Electrochemical Behavior

The electrochemical behavior has been studied in order to observe the potential window and other parameters concerning different active area. The electrochemical responses from non-perforated and perforated diamonds electrodes in 0,1 M KCl solution are shown in Fig. 3. All results are shown in terms of current density by using the geometric area of the samples.

The large potential window can be observed, as expected, for both electrodes. The anodic current density observed from the curve of perforated diamond is around twice higher than non-perforated diamond. This result is probably due to the difference between the real area and the geometric area, for both electrodes, which promote the double layer capacitance increase[20].

In order to verify if the diamond/Ti6Al4V electrodes have the same electrochemical properties of the standard diamond\silicon electrodes, the electrochemical activity at 2 and –2 V of the two diamond/Ti6Al4V electrodes in acid

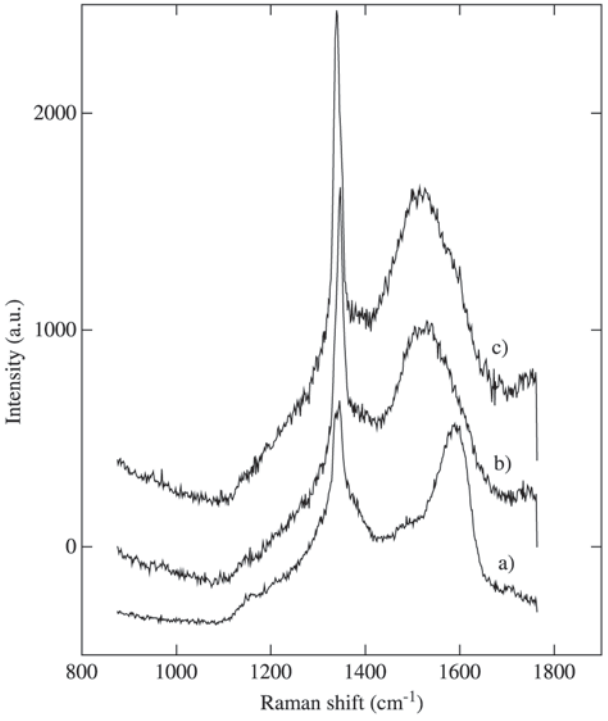

Figure 2. Raman spectra for boron-doped diamond in: a) non-perforated sample; b) between two holes on perforated sample; c) near to a hole on perforated sample.

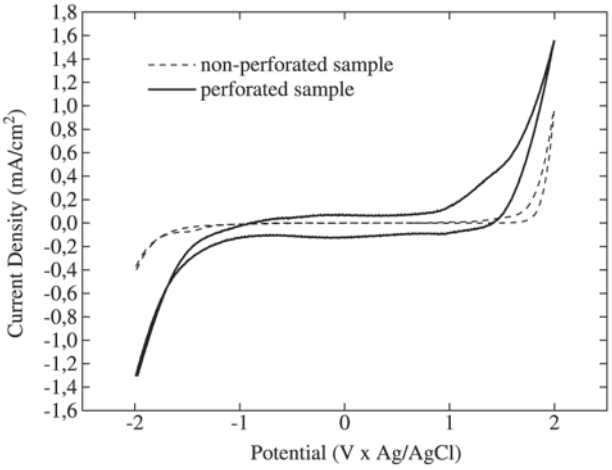

Figure 3. Cyclic voltametric behavior of the electrodes in 0,1 M KCl solution at v=100 mV/s.

and neutral solutions were compared with diamond/silicon doped, as shown in Fig. 4 and 5, respectively[20,21]. The figures show the current densities values of the anodic (I_{max}) and cathodic (I_{min}) reactions, which correspond to oxygen and hydrogen evolution. The values for all electrodes are in miliampere range indicating a coherent response of the electrodes. In the acid solution, the cathodic current density are approximately 10 times larger and anodic are similar to those in neutral solutions, confirming the high sensitivity of the diamond surface to hydrogen, in the form of H^+ ions, as observed by Deneuville *et al.*[21].

The main objective of the next experiments were to verify the electrode response agreement, using some criteria of reversibility[22], for the redox reactions in $K_4Fe(CN)_6$ solution. The results obtained from cyclic voltammetry of $Fe(CN)_6^{3-/4-}$ in 0,1 M KCl solution with perforated boron-doped diamond/Ti6Al4V electrode and boron-doped diamond/Si are shown in Figs. 6-8. The data reported are corrected by IR compensation. The first criterion analyzed was the relation between the cathodic peak current and the square root of the sweeping rate, which is shown in Fig. 6. The data indicate that the Ip increases with the relation sweep rate square in agreement. Other criterion was the separation between the anodic and cathodic peaks that in this case increases with the sweeping rate increase, as shown in Fig. 7. In addition, from Fig. 8, the cathodic peak potential changes to negatives values as a function of the sweeping rate increase. Therefore, all results indicated that $Fe(CN)_6^{3-/4-}$ couple is quasi-reversible at diamond/Ti6Al4V, as at diamond/Si[23].

However one of the conditions to consider the reaction quasi-reversible is that ΔEp values tend to 60 mV (once n is equal 1 in this system) at low sweeping rate. In our case, the higher values found for ΔE_p, including at low sweep rates, and the original forms of the curves suggest that the films

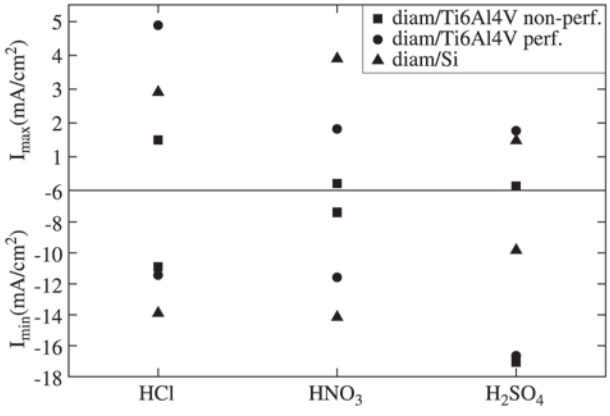

Figure 4. Current density in 0,1 M acid solutions.

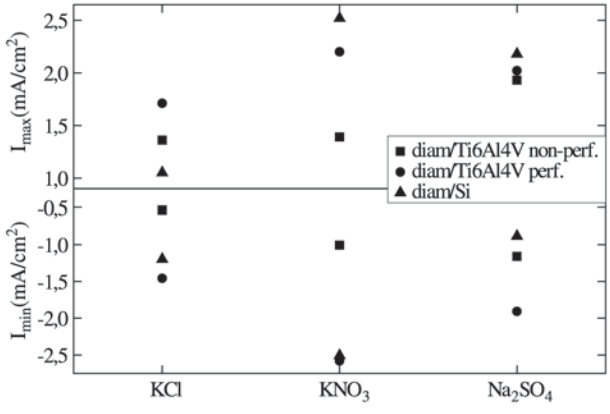

Figure 5. Current density in 0,1 M neutral solutions.

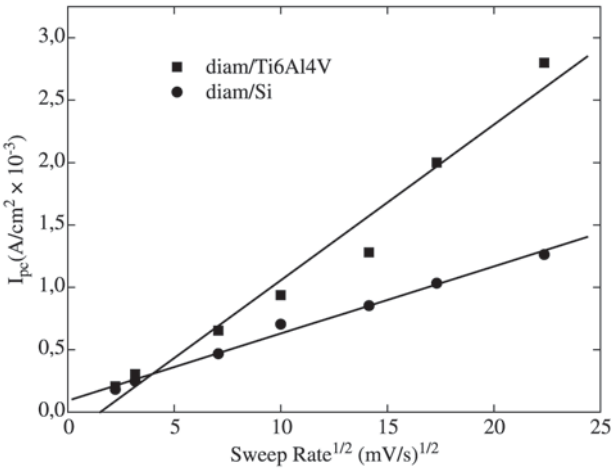

Figure 6. Cathodic peak current as a function of (sweep rate)$^{1/2}$ in 1mM Ferrocyanide/0,1 M KCl for perforated electrode.

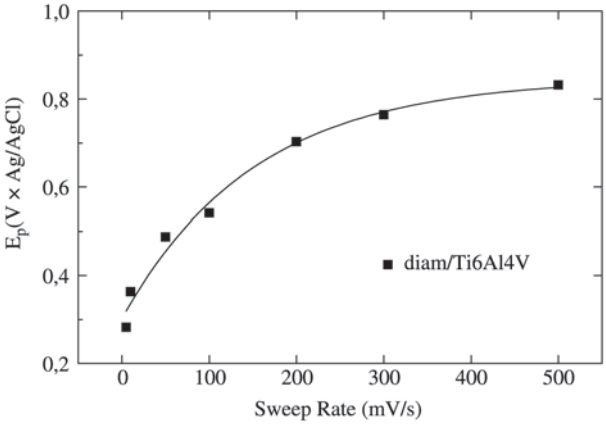

Figure 7. ΔEp as a function of sweep rate in 1 mM Ferrocyanide 0,1 M KCl for perforated electrode.

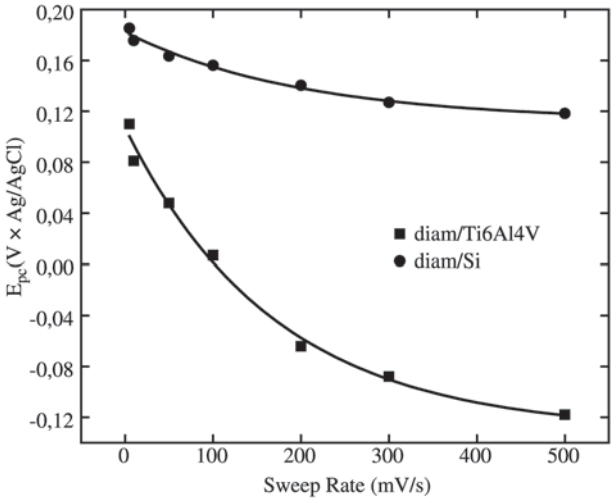

Figure 8. Cathodic potential as a function of sweep rate in 1 mM Ferrocyanide/0,1 M KCl for perforated electrode.

are more resistive or less doped, as described by Ramesham and Rose[24].

4. Conclusion

The thin films of boron-doped diamond were grown on perforated and non-perforated Ti6Al4V samples with good adhesion. SEM and Raman Scattering Spectroscopy characterized their quality and morphology indicating films with small average grain size, highly stressed, slightly doped and with some quantity of sp^2 carbon.

The electrodes electrochemical behavior showed similarity with the standard electrodes deposited on silicon. Although in the perforated samples the double layer capacitance was increased. This behavior turns them suitable for electrochemical capacitors applications. The electrochemical properties, as large potential window, electrochemical activity in different neutral and acid solutions and cyclic voltammetry behavior of the $Fe(CN)_6^{3-/4-}$ at the electrodes, were the expected ones. This is very important to assure good performance in future applications.

Acknowledgements

The authors are very grateful to FAPESP for financial support and to Mr. Jognes Panasiewicz Junior from Instituto Nacional de Pesquisas Espaciais for SEM analyses and Mrs. Maria Auxiliadora S. Oliveira from Instituto Tecnológico de Aeronáutica (ITA) for potentiostat equipment.

References

1. Tsai, W.; Delfino, M.; Ching, L.Y.; Reynolds, G.; Hodul, D.; Cooper, C.B *New Diamond Science and Technology*, MRS Int. Conf. Proc. P. 937, 1991.
2. Prawer, S. *Diamond and Related Material*, v. 4, p. 862, 1995.
3. Martin, H.B.; Argotia, A.; Landau, U.; Anderson A.B.; Angus, J.C. *J. Electrochem. Soc*., v. 143, n. 6, p. 133, 1996.
4. Okano, K.; Akiba, Y.; Kurosu, T.; Lida, M.; Nakamura, T. *J. Cristal Growth*, v. 99, p. 1192, 1990.
5. Tenne, R.; Lévy-Clément, C. *Israel Journal of Chemistry*, v. 38, p. 57-73, 1998.
6. Fisher, V.; Gandini, D.; Laufer, S.; Blank, E.; Comninellis, C. *Electrochimica Acta*, v. 44, p. 521-524, 1998.
7. Peng, X.L.; Clyne, T.W. *Thin Solid Films*, v. 293, p. 264-269, 1997.
8. Silva, L.L.G.; Corat, E.J.; Barros, R.C.M.; Trava-Airoldi ,V.J.; Leite, N.F.; Iha, K. *Materials Research*, v. 2, n. 2, p. 99-103, 1999.
9. Ferreira, N. G.; Abramof, E.; Corat, E.J.; Leite, N.F.; Trava-Airoldi, V.J. *Diamond and Related Materials*, v. 10, p. 750-754, 2001.
10. Fan, W.D; Jagannadham, K.; Narayan, J. *Surface and Coatings Tecnology*, v. 91, p. 32-36, 1997.
11. Rats, D.; Vandenbulcke, L.; Serin, V.; Sevely, J. *Thin Solid Films*, v. 270, p. 177-183, 1995.
12. Vandenbulcke, L.; Rats, D.; Herbin, R. *Materials Letters*, v. 27, p. 77-80, 1996.
13. Scardi, P.; Leoni, M.; Cappuccio, G.; Sessa, V.; Terranova, M.L. *Diamond and Related Materials*, v. 6, p. 807, 1997.
14. Perry, S.S.; Ager, J.W.; Somorjai, G.A. *J. Appl. Phys*, v. 74, p. 7542-7550, 1993.
15. Knight, D.S; White, W.B. *J. Mater. Res*, v. 4, n. 2, p. 385-393, 1989.
16. Nemanich, R.J.; Glass, J.T.; Lucovsky, G.; Shroder, R.E. *J. Vac. Sci. Technol*. A, v. 6, p. 1783-1787, 1988.
17. Gheeraert, E.; Deneuville, A.; Bonnot, A.M. *Diamond and Related Materials*, p. 525-528, 1992.
18. Wang, W.L.; Pólo, M.C.; Sanchez, G.; Esteve, J. *J. Appl. Phys*, v. 80, p. 1846-1850, 1996.
19. Liao, X.Z.; Zhang, R.J.; Lee, C.S.; Lee, S.T.; Lam, Y.W. *Diamond and Related Materials*, v. 6, p. 521-525, 1997.
20. Ferreira, N.G.; Silva, L.L.G.; Corat, E.J. *Diamond Related Materials*, v. 11, p. 657-661, 2002.
21. Lévy-Clément, C.; Zenia, F.; Ndao, N.A.; Deneuville, A. *New Diamond and Frontier Carbon Technology*, v. 9, n. 3, p.189-206, 1999.
22. Greef, R.; Peat, R.; Peter, L.M.; Pletcher, D.; Robinson, J. *Instrumental Methods in Electrochemistry*, John Wiley & Sons, New York, cap. 3, 1985.
23. Ferreira, N.G.; Silva, L.L.G.; Corat, E.J. in press.
24. Ramesham, R.; Rose, M.F. *Diamond Related Materials*, v. 6, p. 17-27, 1997.